

# Determining the Trajectory of the Crane Block Using the Finite Element Method

## Određivanje putanje koloturnika kuke dizalice koristeći se metodom ograničenog elementa

Andrzej Grządziela

Polish Naval Academy  
Faculty of Mechanical & Electrical  
Engineering  
Gdynia, Poland  
E-mail: a.grzadzela@amw.gdynia.pl

Radosław Kiciński\*

Polish Naval Academy  
Faculty of Mechanical &  
Electrical Engineering  
Gdynia, Poland  
E-mail: r.kicinski@amw.gdynia.pl

Bogdan Szturomski

Polish Naval Academy  
Faculty of Mechanical &  
Electrical Engineering  
Gdynia, Poland  
E-mail: bsztur@gmail.com

Paweł Piskur

Polish Naval Academy  
Faculty of Mechanical & Electrical  
Engineering  
Gdynia, Poland  
E-mail: p.piskur@amw.gdynia.pl

DOI 10.17818/NM/2022/2.3

UDK 621.85.055.4 : 531.1

Review / Pregledni rad

Paper received / Rukopis primljen: 14. 12. 2021.

Paper accepted / Rukopis prihvaćen: 20. 4. 2022.

### Abstract

The paper discusses determining crane block trajectories using the finite element method (FEM). The mathematical formulation for air resistance of hooks' block is presented with kinematic analysis of the block. The three crane blocks are considered: without wind deflector, with a spherical deflector and a cylindrical fairing. The hook block was assumed as a physical pendulum. The FEM analysis is provided with the hook block movement consideration. Movement trajectories of hook blocks for different wind speeds is depicted and the results are. At the end of the paper, the conclusions are provided with the directions of future research.

### Sažetak

U ovom radu raspravlja se o određivanju putanje koloturnika dizalice koristeći se metodom ograničenog elementa (FEM). Matematička formulacija za otpor zraka koloturnika kuke dizalice prikazuje se kinematičkom analizom koloturnika. Promatraju se tri koloturnika dizalice: bez deflektora vjetrova, sa sferičnim deflektorom i cilindričnom oplatom. Koloturnik kuke uzima se kao fizičko njihalo. FEM analiza temelji se na promatranju gibanja koloturnika kuke. Oslikava se putanja gibanja koloturnika kuke za različite brzine vjetrova i iznose se rezultati. Na kraju rada predočavaju se zaključci sa smjernicama za buduća istraživanja.

### KEY WORDS

gantry crane  
hooks' block  
trajectory  
simulations  
FEM

### KLJUČNE RIJEČI

velika dizalica  
koloturnik kuka  
putanja  
simulacije  
FEM

## 1. INTRODUCTION / Uvod\*

The port cranes and gantry cranes used today have increased load capacity. The increase in load capacity requirements applies to crane handling in commercial ports and devices at production and repair sites. The conditions apply to shipyards executing orders in sea production and wind energy. High capacity crane designs appear to be a widely offered portfolio of key manufacturers around the world today. One of the main problems of giant gantry cranes is wind. Safety regulations limit the participation of people during loading or unloading to wind speeds above 12 m / s. In high capacity gantry cranes, wind speeds even lower than 12 m / s can cause problems or even a threat to the dynamic positioning of the hook block over the load. The average wind speed on the South Baltic coast is 9 m / s, indicating real operational problems [1].

The shipbuilding industry often uses modular technologies that ensure fast production rates, high quality, and timely systems deliveries. The modules of the shipping system are elements whose weight ranges from several dozen kilograms to 500 or more tons. Assembling such large-size parts for sea or offshore ships is a big logistic challenge. The gantry crane can handle extensive, irregularly shaped structure components

produced and transported in shipyards. The safety regulations indicate that the personnel engaged in loading or unloading the gantry crane limits their activities to the average wind speed over the entire height of the crane to 12 m / s. Dynamic impacts related to the irregularity of the gust of wind and the change of its direction prevent precise lowering of the lifting mechanism with the hook and ropes [2,3]. Another significant problem is lifting the module with a larger surface than the hook block and crane ropes.

Analyzing the above, the idea of remote control of the block using the appropriate numerical control emerged. A proper test should be carried out to achieve this concept, and mathematical models developed that will cause the block to move onto the automatic hook in due time. To determine the moment of lowering the automatic hook onto the catch, numerical tools should be prepared. The trajectories of the block movement should be initially determined depending on the strength and direction of the wind.

## 2. OBJECT OF RESEARCH / Cilj istraživanja

The paper presents a numerical analysis of the trajectory of the hook block movement subjected to variable wind influences. The

\* Corresponding author

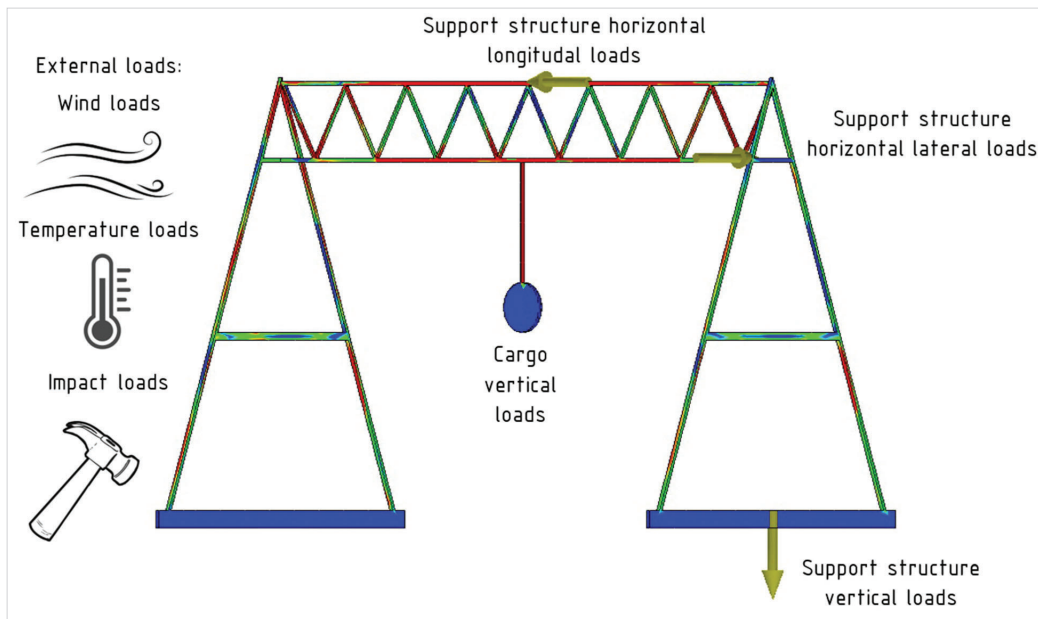


Figure 1 Structure of loads acting on the gantry crane  
Slika 1. Struktura opterećenja koja djeluju na jaku dizalicu

Source: Authors

same block equipped with a fairing that reduces aerodynamic drag has been simulated. The simulation results were calculated for the crane with the main girder at the height of 30 m. The research object is a gantry crane with a lifting capacity of up to 50 tons, which is in the conceptual design phase. The primary technical parameters are presented below:

- height of the crane leg – 30 m,
- width of the crane bridge – 38 m,
- weight of the maximum load – 50 t,
- number of wire ropes – 6,
- number of legs – 4.

Lifting cargo with a weight of up to 50 tons requires a substantial construction of all elements, starting from the frame structure, crane bridge, crab and ending with the wire rope, hook block and finally, the hook. The basic assumption is the correct analysis of the existing static and dynamic loads [4]. The results of the preliminary study are presented in Figure 1.

It was assumed that a block under the influence of wind behaves like a physical pendulum. The mass of the four slings and their stiffness were taken, where is  $k = 1250 \text{ N/m}$ . The hook's block surfaces were determined from the CAD documentation, as were the cylindrical and spherical fairing surfaces. The simulations neglect the effect of the torsional moment of the stretched rope. This assumption is justified by the wire rope slings construction presented in Figure 2 [5].

The core is the centre of the wire rope and serves as the foundation to hold the rope together. There are three cores, i.e. fibre, strand or Independent Wire Rope (IWR). The basic unit of the wire rope is the wire, mainly made from carbon steel. Finally, the cross lay strand is called a specific number of wires laid helically around a wire core. Spiral ropes can be dimensioned so that they are non-rotating, so under tension, the rope torque is almost zero.

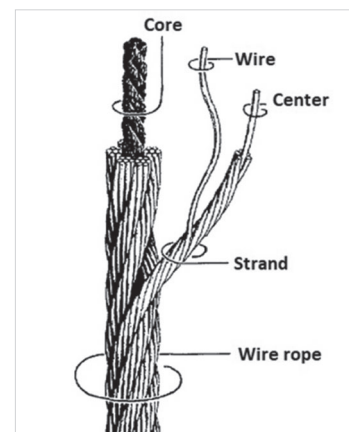


Figure 2 Construction of the wire rope slings  
Slika 2. Konstrukcija čeličnog užeta

Source:[5]

### 3. AIR RESISTANCE OF HOOKS' BLOCK AND WIND DEFLECTORS / Otpor koloturnika kukâ i deflektori vjetra

The aerodynamic force is the resultant of elemental forces exerted on the surface of a solid by the flowing fluid. The throw of force to the direction of velocity is called aerodynamic drag. In balanced flow, the aerodynamic drag consists of:

- pressure resistance, also called shape resistance (projection of normal in the direction  $\vec{V}_{\infty}$ )

$$P_{xc} = \iint_S p \vec{n} \cos(-\vec{n}, \vec{V}_{\infty}) ds \quad (1)$$

where  $\vec{n}_i$  - normal external of the arc element  $ds$  (see Figure 3),

- frictional resistance (projection of the tangents in the direction of  $\vec{V}_{\infty}$ )

$$P_{xt} = \iint_S \vec{\tau} \cos(\vec{s}, \vec{V}_{\infty}) ds \quad (2)$$

where by  $\vec{s}, \vec{V}_\infty$  is understood the angle between the tangent to the profile having this same turn as  $\vec{\tau}$ , and the direction of velocity  $\vec{V}_\infty$ .

Their sum is the profile resistance, often called drag force:

$$P_x = P_{xc} + P_{xt} \quad (3)$$

The mutual share of pressure and frictional resistance in the profile resistance depends on the body's shape, its orientation concerning the flow direction, and the flow's nature in the boundary layer. For example, for a flat plate perpendicular to the velocity direction, the pressure resistance is the entirety of the aerodynamic drag. For the same plate placed in parallel, the pressure resistance is zero, and the profile resistance is equal to the frictional resistance. Sometimes the total resistance may be even slightly lower than the pressure resistance, as part of the contour is draped in the opposite direction to the resultant force  $P_x$ . Generally, it is assumed that "streamlined" shapes are those for which frictional resistance is the central part of the aerodynamic drag, and "non-streamlined" bodies are those for which frictional resistance is negligible compared to pressure resistance. Aerodynamic forces, and hence drag, can be measured by the following methods:

- 1) using the principle of conservation of momentum,
- 2) using the measurement of pressure distribution and tangential stress on the surface of the flowing body,
- 3) by weight (direct force measurement).

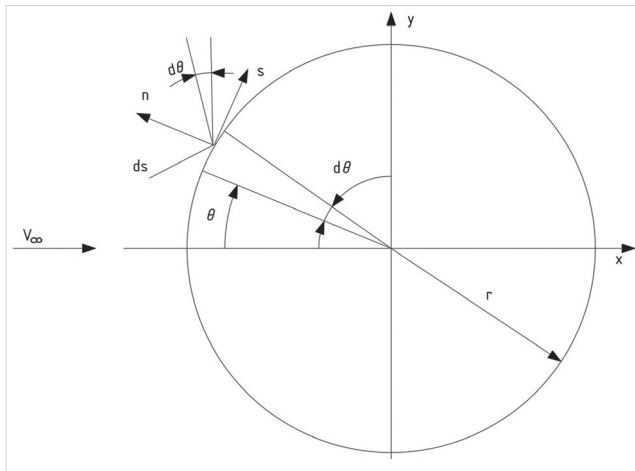


Figure 3 Coordinate system  
Slika 3. Sustav koordinata

Source: Authors

It is accepted in the paper that "streamlined" shapes are those for which frictional resistance is the major part of the aerodynamic drag, and "non-flowing" bodies are those for which frictional resistance is negligible compared to pressure resistance. For simulation, the principle of conservation of momentum was adopted in work.

#### 4. KINEMATICS ANALYSIS OF THE HOOKS' BLOCK / Kinematička analiza koloturnika kukâ

The shipyard crane modelling methods were presented in the paper [6], where the effect of wind force on the dynamic of shipyard cranes, particularly on hook movements in

the horizontal plane was discussed. The Cartesian system uniquely assigns the coordinates of each point in space. In the description of the physical pendulum rotation dynamics for the vertical position, the sine of the angle takes the value zero. For mathematical pendulum description, where the sine of the angle is in the denominator of the equation, it leads to ambiguity of the solutions. Therefore, a spherical coordinate system with a selected frame of reference was used in further analysis (see Figure 4).

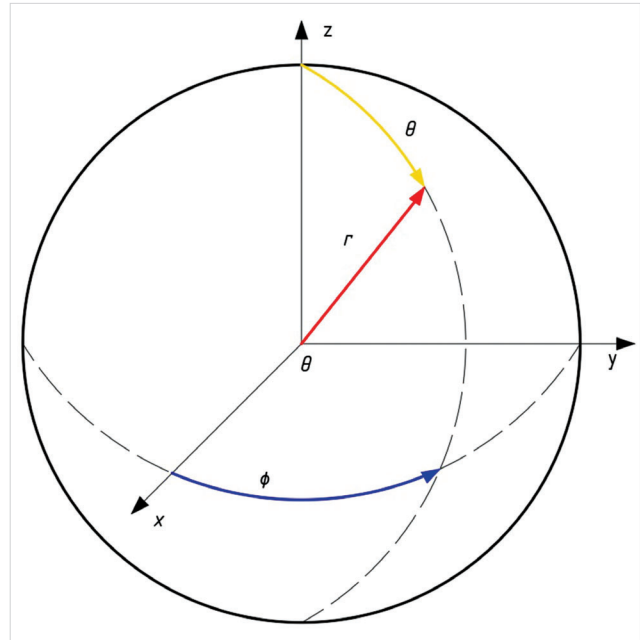


Figure 4 Spherical coordinate system  
Slika 4. Sustav sferičnih koordinata

Source: Authors

To any point,  $M$  is assigned its spherical coordinates:

- leading radius  $r \geq 0$ , i.e. the distance of point  $M$  from the origin of the system  $O$ ,
- length  $0 \leq \phi < 2\pi$ , i.e. the measure of the angle between the rectangular projection of the vector  $OM$  onto the  $Oxy$  plane and the positive half-axis  $Ox$ .
- the distance  $0 \leq \theta \leq \pi$ , i.e. the measure of the angle between the vector  $OM$  and the positive semi-axis  $Oz$ ,

The relationship between the Cartesian coordinate system and the spherical coordinate system can be written using equation (1).

$$\begin{aligned} x &= x(r, \theta, \phi) = r \sin \theta \cos \phi \\ y &= y(r, \theta, \phi) = r \sin \theta \sin \phi \\ z &= z(r, \theta, \phi) = r \cos \theta \end{aligned} \quad (4)$$

Similarly, for the adopted Cartesian coordinate system, the block coordinates  $(x_c, y_c, z_c)$  can be written, based on Figure 4, using the equation (5):

$$\begin{cases} x_c = R \cos(\alpha) \\ y_c = R \sin(\alpha) \sin(\beta) \\ z_c = -R \sin(\alpha) \cos(\beta) \end{cases} \quad (5)$$

The minus in the third equation (5) results from the adopted orientation of the  $z$ -axis. One should pay attention to the change of the coordinate system. The difference is caused by the need to avoid singular solutions that occur for small inclination angles of the crane block in inverse kinematics. This means that

if the coordinate system was adopted as in Figure 5, where the projection of the R-length line is realized on the 0xy plane, for small block deflection angles, the sine value would be close to zero, which in some equations would result in dividing by zero.

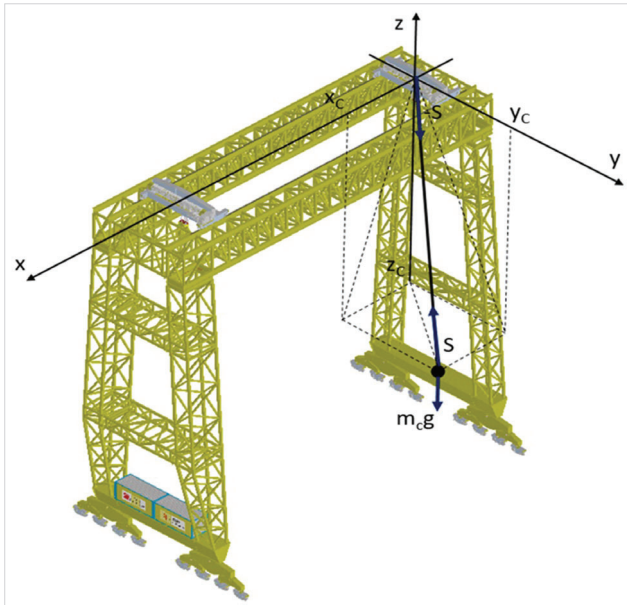


Figure 5 Cartesian coordinate system on the crane - isometric view  
Slika 5. Kartezijanski sustav koordinata na dizalici – izometrički pogled

Source: Authors

The change of the spherical coordinate system consists of projecting the line on the 0yz plane [7]. For the coordinate system adopted in this way, the block near the equilibrium point will occur for the angle  $\alpha$  approximating 90 degrees, i.e.  $\pi/2$  radians. Of course, the sine of the angle  $\alpha$  for small angles will still be close to zero, but such a position will correspond to the forbidden states of the crane, i.e. those for which the pulley would be located in the horizontal plane.

Newton's second law of dynamics was used to present the dynamics of the gantry elements based on which the following equations:

$$\begin{aligned} F_x &= a_x(m_w + m_c) \\ F_y &= a_y(m_s + m_w + m_c) \\ F_R &= a_R m_c \end{aligned} \quad (6)$$

The above equations describe the crane dynamics taking into account the mass of the block  $m_c$ , the mass of the crab  $m_w$  and the mass of the gantry frame  $m_s$ . The following forces' formulas were adopted:

- $F_x$  - the force acting on the drives along the x-axis;
- $F_y$  - the force acting on the drives along the y-axis;
- $F_R$  - the force acting on the drives along the ropes of length R.

The friction force should be included in the description of the crane dynamics. Friction is defined as the relationship directly proportional to the friction coefficient  $\mu_T$  and the contact force  $F_T$ .

$$F_T = \mu_T F_N \quad (7)$$

The pressure force is proportional to the weight of the crane components. The gantry dynamics depends on the friction force and the mass of the gantry crane elements according to the following relationship:

$$\begin{aligned} T_x &= a_1(m_w + m_c) \\ T_y &= a_2(m_c + m_w + m_s) \\ T_R &= a_3 m_c \end{aligned} \quad (8)$$

where:

- $T_x$  - is the frictional (drag) force along the x-axis;
- $T_y$  - is the frictional (drag) force along the y-axis;
- $T_R$  - is the frictional (drag) force along the rope's axis on which the hook block is suspended.

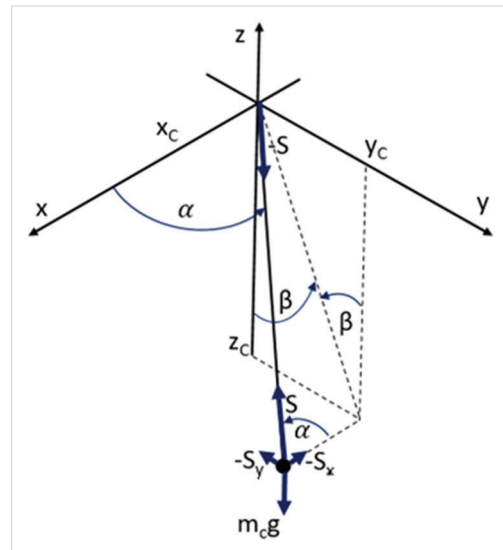


Figure 6 Forces acting on the block  
Slika 6. Sile koje djeluju na koloturnik

Source: Authors

The dynamics of the hooks block (Figure 6) can be written as follow:

$$\begin{aligned} S_x &= m_c \ddot{x}_c \\ S_y &= m_c \ddot{y}_c \\ S_z &= m_c \ddot{z}_c + m_c g \end{aligned} \quad (9)$$

The gantry crab dynamics (taking into account the dynamics of the block ( $m_c$ ) and the mass of the gantry  $m_g$ , which is rigidly connected to the crab) can be written:

$$S_x - F_x = m_w \ddot{x}_w \quad (10a)$$

$$S_y - F_y = (m_w + m_s) \ddot{y}_w \quad (10b)$$

Equations (10) do not contain the equation of forces for the z-axis as the carriage does not travel vertically. The components of the force  $S_x, S_y, S_z$  of the rope's interaction with the trolley can be determined from the angular relations (Figure 6):

$$\begin{aligned} S_x &= S \cos(\alpha) \\ S_y &= S \sin(\alpha) \sin(\beta) \\ S_z &= -S \sin(\alpha) \cos(\beta) \end{aligned} \quad (11)$$

In equations (11), the components of the forces  $S_x, S_y, S_z$  are considered from the crab side. Therefore  $S_x, S_y$  have returns consistent with the x- and y-axes, while  $S_z$  is opposite to the z-axis. The equations assume that the rope is always tight. The force vector of the pulley acts on the crab, and it is directed from the crab towards the load.

$$S_x(x_c - x_w) + S_y(y_c - y_w) + S_z z_c > 0 \quad (12)$$

Assuming that the deviation of the rope from the vertical axis is slight, the trigonometric values of the angles can be written in a simplified form:

$$\cos(\alpha) = \cos\left(\frac{1}{2}\pi + \alpha\right) \cong -\alpha \quad (13)$$

$$\sin(\alpha) = \sin\left(\frac{1}{2}\pi + \alpha\right) \cong 1 \quad (14)$$

$$\cos(\beta) \cong 1 \quad (15)$$

$$\sin(\beta) \cong \beta \quad (16)$$

The system of equations (9) on the basis of simplifications (13) - (16) can be written:

$$\begin{aligned} S_x &= -S\alpha \\ S_y &= S\beta \\ S_z &= -S \end{aligned} \quad (17)$$

Substituting the above dependencies (17) into the dynamics equations of the block (9), it obtains the following relations:

$$S_x = -S\alpha \quad S_x = m_c \ddot{x}_c \quad \rightarrow \quad -S\alpha = m_c \ddot{x}_c \quad (18)$$

$$S_y = S\beta \quad S_y = m_c \ddot{y}_c \quad \rightarrow \quad S\beta = m_c \ddot{y}_c \quad (19)$$

$$S_z = -S \quad S_z - m_c g = m_c \ddot{z}_c \quad \rightarrow \quad -S - m_c g = m_c \ddot{z}_c; \quad (20)$$

After transformations:

$$\ddot{x}_c = \frac{-S\alpha}{m_c} \quad (21)$$

$$\ddot{y}_c = \frac{S\beta}{m_c} \quad (22)$$

$$\ddot{z}_c = \frac{S}{m_c} - g \quad (23)$$

Taking into account the system of equations (6) and the simplifications of the trigonometric values of the angles, it results:

$$\begin{cases} x_c = x_w - R\alpha \\ y_c = y_s + R\beta \\ z_c = -R \end{cases} \quad (24)$$

By differentiating the above system of equations over time, we obtain dependencies on the hook block speed:

$$\begin{cases} \dot{x}_c = \dot{x}_w - (\dot{R}\alpha + R\dot{\alpha}) \\ \dot{y}_c = \dot{y}_s + (\dot{R}\beta + R\dot{\beta}) \\ \dot{z}_c = -\dot{R} \end{cases} \quad (25)$$

By differentiating again over time, we get a system of the hook block acceleration equations:

$$\begin{cases} \ddot{x}_c = \ddot{x}_w - (\ddot{R}\alpha + \dot{R}\dot{\alpha} + \dot{R}\dot{\alpha} + R\ddot{\alpha}) \\ \ddot{y}_c = \ddot{y}_s + (\ddot{R}\beta + \dot{R}\dot{\beta} + \dot{R}\dot{\beta} + R\ddot{\beta}) \\ \ddot{z}_c = -\ddot{R} \end{cases} \quad (26)$$

after adding the same components, equation (26) takes the final form:

$$\begin{cases} \ddot{x}_c = \ddot{x}_w - (\ddot{R}\alpha + 2\dot{R}\dot{\alpha} + R\ddot{\alpha}) \\ \ddot{y}_c = \ddot{y}_s + (\ddot{R}\beta + 2\dot{R}\dot{\beta} + R\ddot{\beta}) \\ \ddot{z}_c = -\ddot{R} \end{cases} \quad (27)$$

By inserting dependencies from equation (27) into equations (21-23):

$$\begin{cases} \ddot{x}_c = \frac{-S\alpha}{m_c} \\ \ddot{y}_c = \frac{S\beta}{m_c} \\ \ddot{z}_c = \frac{S}{m_c} - g \end{cases}$$

and:

$$\begin{cases} \ddot{x}_w - (\ddot{R}\alpha + 2\dot{R}\dot{\alpha} + R\ddot{\alpha}) = \frac{-S\alpha}{m_c} \\ \ddot{y}_s + (\ddot{R}\beta + 2\dot{R}\dot{\beta} + R\ddot{\beta}) = \frac{S\beta}{m_c} \\ -\ddot{R} = \frac{S}{m_c} - g \end{cases} \quad (28)$$

after removing the parentheses:

$$\begin{cases} \ddot{x}_w - \ddot{R}\alpha - 2\dot{R}\dot{\alpha} - R\ddot{\alpha} = \frac{-S\alpha}{m_c} \\ \ddot{y}_s + \ddot{R}\beta + 2\dot{R}\dot{\beta} + R\ddot{\beta} = \frac{S\beta}{m_c} \\ -\ddot{R} = \frac{S}{m_c} - g \end{cases} \quad (29)$$

By isolating the unknown output variables, we obtained:

$$\begin{cases} \ddot{\alpha} = \frac{1}{R} \left( \frac{S\alpha}{m_c} - \ddot{x}_w + \ddot{R}\alpha + 2\dot{R}\dot{\alpha} \right) \\ \ddot{\beta} = \frac{1}{R} \left( \frac{S\beta}{m_c} - \ddot{y}_s - \ddot{R}\beta - 2\dot{R}\dot{\beta} \right) \\ \ddot{R} = g - \frac{S}{m_c} \end{cases} \quad (30)$$

By adding to the above equations two equations describing the dynamics of the crab (10):

$$\begin{cases} S_x - F_x = m_w \ddot{x}_w \\ S_y - F_y = (m_w + m_s) \ddot{y}_w \end{cases}$$

and transforming concerning unknown values it gets:

$$\begin{cases} \ddot{x}_w = \frac{1}{m_w} (S_x - F_x) \\ \ddot{y}_w = \frac{1}{m_w + m_s} (S_y - F_y) \end{cases} \quad (31)$$

Combining equations (30) and (31), it gets five second-order nonlinear equations:

$$\begin{cases} \ddot{\alpha} = \frac{1}{R} \left( \frac{S\alpha}{m_c} - \ddot{x}_w + \ddot{R}\alpha + 2\dot{R}\dot{\alpha} \right) \\ \ddot{\beta} = \frac{1}{R} \left( \frac{S\beta}{m_c} - \ddot{y}_s - \ddot{R}\beta - 2\dot{R}\dot{\beta} \right) \\ \ddot{R} = g - \frac{S}{m_c} \\ \ddot{x}_w = \frac{1}{m_w} (S_x - F_x) \\ \ddot{y}_w = \frac{1}{m_w + m_s} (S_y - F_y) \end{cases} \quad (32)$$

The input data are the forcing forces  $F_x$ ,  $F_y$  and  $S$ , and the output data are the vertical position of the rope with the hook block and the horizontal position of the crab. The hook block and crane weights, as well as the acceleration due to gravity, are constant.

The study considered three hook blocks, i.e. without wind deflector, with a spherical deflector and a cylindrical fairing (Figure 7). The hook block under wind loads will move a different trajectory depending on the variant.

The first stage of calculations determines the air pressure force on the hook block. This force is equal to the

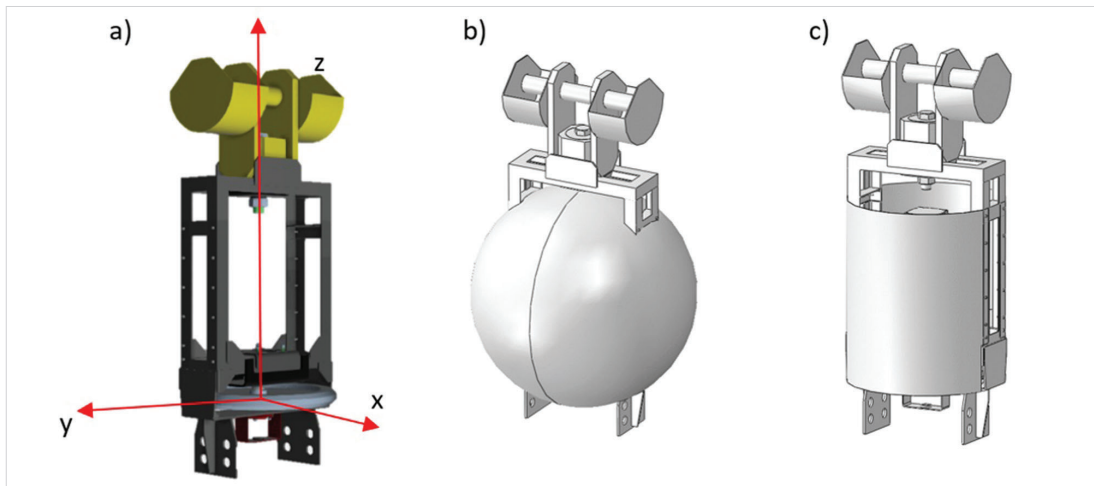


Figure 7 Hook block in various configurations a) without deflector, b) with a spherical deflector, c) with a cylinder-shaped fairing  
 Slika 7. Koloturnik kuke u različitim konfiguracijama: a) bez deflektora, b) sa sferičnim deflektorom, c) s oplatom u obliku cilindra

Source: Authors

air resistance acting on the block and takes the following form [8]:

$$R_A = C_A \rho_p \frac{v_p^2}{2} A_z \quad (33)$$

where:

- $\rho_p$  is the air density in  $\text{kg/m}^3$ ,
- $v_p$  is the wind speed in  $\text{m/s}$ ,
- $A_z$  is the area of the block's transverse projection to the wind direction in  $\text{m}^2$ ,
- $C_A$  is the coefficient of air drag.

Based on the anemometer research, it was assumed that the wind amplitude changes according to the formula:

$$R_W = R_A + 0,15R_A \sin(0,2 \cdot t) \quad (34)$$

and that the wind in the horizontal plane  $xOy$  changes its direction according to the formula:

$$\begin{aligned} R_{WX} &= R_W \sin(0,8t) \\ R_{WY} &= R_W \cos(0,8t) \end{aligned} \quad (35)$$

According to the formula (33), the surface area on which the wind acts depending on the direction should be determined. The coordinate system and the directions of wind action were determined, and then the loads were assumed following the formulas (34), (35). The area of the wind force was determined using CAD (Computer-Aided Design) tools. In the case under consideration, for a block without fairings, the surface area for two directions of wind load should be determined; in the case of using symmetric fairings, the cross-sectional area does not change regardless of the force's direction (Figure 8).

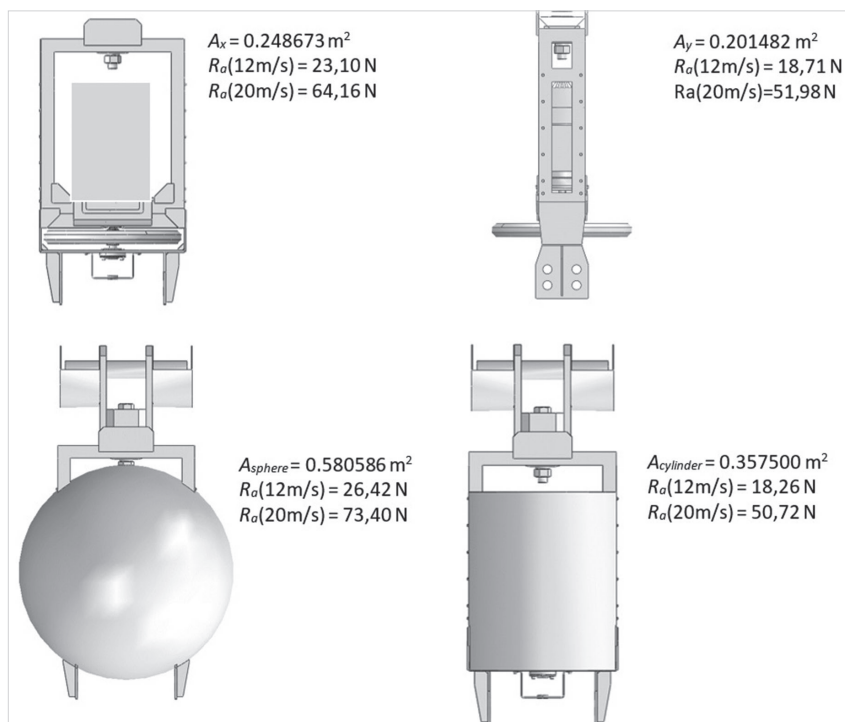


Figure 8 Surface areas and forces acting on hook blocks (the typical block, sphere fairing and cylinder deflector) depend on the wind force  
 Slika 8. Prostori površina i sile koje djeluju na koloturnik kuke (tipični koloturnik, sferična oplata i cilindrični deflektor) ovise o snazi vjetra

Source: Authors

After calculating the block area in various fairing configurations, based on the literature [9], the values of the air resistance coefficients were determined:

- $C_{A-Z}$  – drag coefficient for the hook block = 1,
- $C_{A-W}$  – drag coefficient for a cylinder deflector = 0,55,
- $C_{A-K}$  – drag coefficient for a sphere fairing = 0,49.

Then, the forces generated by the wind for two wind speeds (12 and 20 m/s) were determined, depending on its direction of operation (Figure 9).

This force changes its value in two directions ( $x, y$ ) according to (33), so the block will move along a specific trajectory. The hook block can be considered as a physical pendulum (Figure 10). Thus, the amplitudes and trajectories of motion can be determined using the appropriate mathematical description presented. Finite Element Method (FEM) program support engineering calculations to determine the block moments of inertia and equations of motion. In the case of uniform wind, the pendulum will move along a trajectory close to an ellipse. However, in the proposed model, both the value and the direction of force application change, which will affect the trajectory.

The wind loads the hook block. It will behave like a cycloidal pendulum, i.e. a pendulum. A thread or elastic suspension element will wrap around a cycloid with a horizontal axis and a radius equal to a quarter of the pendulum's length [10]. The problem of a pendulum with an amplitude-independent period comes down to determining such a curve that the body, moving along it under the action of the constant force of gravity, will move from the starting point to its lowest point at the same time. The curve is called a tautochrone and is a cycloid.

To obtain reliable model, the measurements of the dynamics of the sheave block of crane with high lifting capacity was carried out during the wind condition and presented in paper [11]. The precise geodetic devices with appropriate geodetic alignment algorithms was used with positioning errors at the level of several millimetres.

The problem of pendulum motion can be solved by approximating the sine function to two terms, then the equation of pendulum motion takes the form:

$$\frac{d^2\theta}{dt^2} + \frac{g}{l} \left( \theta - \frac{1}{6}\theta^3 \right) = 0 \quad (36)$$

The solution to the above equation has approximately the form (with the accuracy of terms of the 3rd order):

$$\theta(t) = \theta_0 \cos(\omega t) + \theta_3 \cos(3\omega t) \quad (37)$$

where:

- $\theta_0$  - vibration amplitude with a frequency of  $\omega$ ,
- $\theta_3 = \frac{1}{3} \left( \frac{\theta_0}{4} \right)^3$  - vibration amplitude with a frequency of  $3\omega$ ,
- $\omega_0 = \sqrt{\frac{g}{l}}$ ,
- $\omega = \omega_0 \left( 1 - \frac{\theta_0^2}{16} \right)$ .

Substituting the wind model for amplitude can obtain the cycloid equation described in the general case by the parametric equation:

$$\begin{aligned} x &= rt - c \cdot \sin t \\ y &= rt - c \cdot \cos t \end{aligned} \quad (38)$$

The dependence of the distance  $c$  of the point marking the curve on the centre of the rolling circle and the radius  $r$  of this circle is as follows:

- for  $c < r$ , a shortened cycloid, defined by a fixed point lying inside a rolling circle;
- for  $c > r$ , an elongated cycloid defined by a fixed point lying outside the circle;
- for  $c = r$ , a normal cycloid drawn by a point on the edge of the circle.

Depending on the strength of the wind at a given moment in time,  $c$  and  $r$  take different values. Thus, after substituting all dependencies, the approximate trajectory of the block for different wind speeds can be determined.

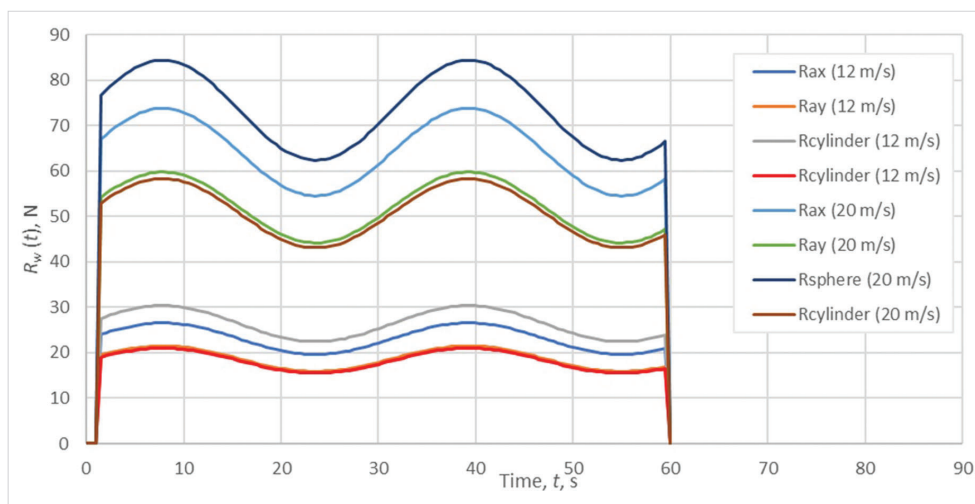


Figure 9 Change of the maximum values of the wind force depending on the hook block variant  
Slika 9. Izmjena maksimalnih vrijednosti snaga vjetra koje ovise o varijanti koloturnika kuke

Source: Authors

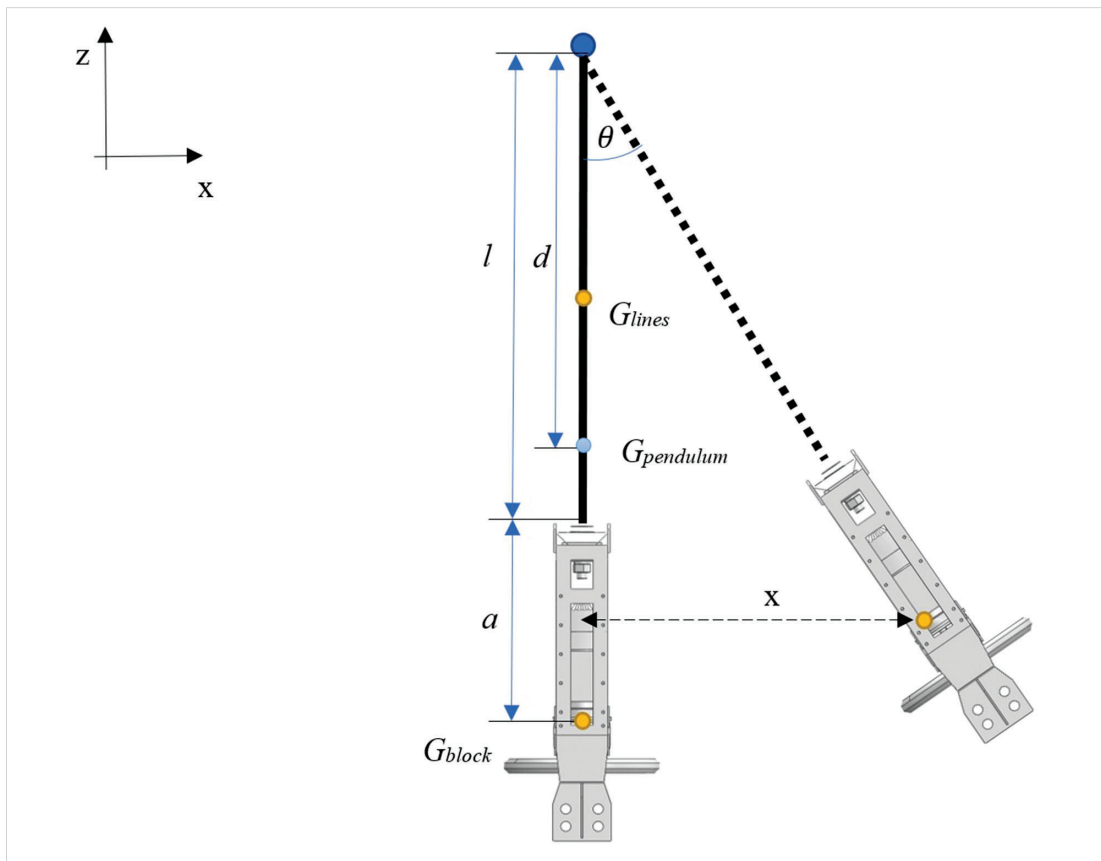


Figure 10 The hook block as a physical pendulum.  
Slika 10. Koloturnik kuke kao fizičko njihalo

Source: Authors

Determining the trajectory of the hook block is a challenge for analytical calculations, therefore in these considerations, it was decided to use FEM (finite element method) to determine the trajectories.

### 5. FEM ANALYSIS OF THE MOVEMENT OF THE HOOK BLOCK / FEM analiza gibanja koloturnika kuke

As rope modelling is a complicated issue, some simplifications have been used in the presented approach. The first is the use of beam elements as perfectly rigid bodies to model the rope. This approach is justified when heavy loads are hanging on the ropes. The mass of the block is 102.5 kg, so it can be assumed that the above statement is correct. Moreover, the forces acting on the block were determined directly from the formulas, so it is unnecessary to model the entire block. Hence the movement of the pendulum comes down to the analysis of a material point suspended on an inelastic thread. The centre of gravity of the physical pendulum, taking into account the rope weight, was determined to be 12 m.

The next step was to determine the block trajectory depending on the input value. The wind load was 60 s, and then for the following 180 s, the traffic of the hook block - the centre of gravity was analyzed (240 s in total). The results are presented for two input speeds, 12 m/s and 20 m/s, for three variants of the block structure. The case-by-case trajectory of the hook blocks is shown below.

The analysis of the trajectory of the centre of gravity of the hook block indicates that the most effective solution is the use of cylindrical fairing. The symmetrical shape, low roughness

and small surface area effectively reduce wind speeds on the hook block for both analyzed wind speeds.

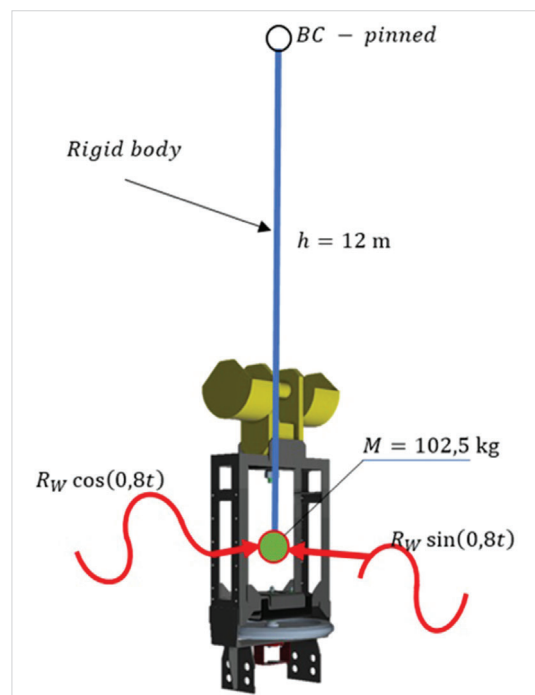


Figure 11 Boundary conditions and load diagram in the FEM simulation

Slika 11. Granični slučajevi i dijagram opterećenja pri FEM simulaciji

Source: Authors

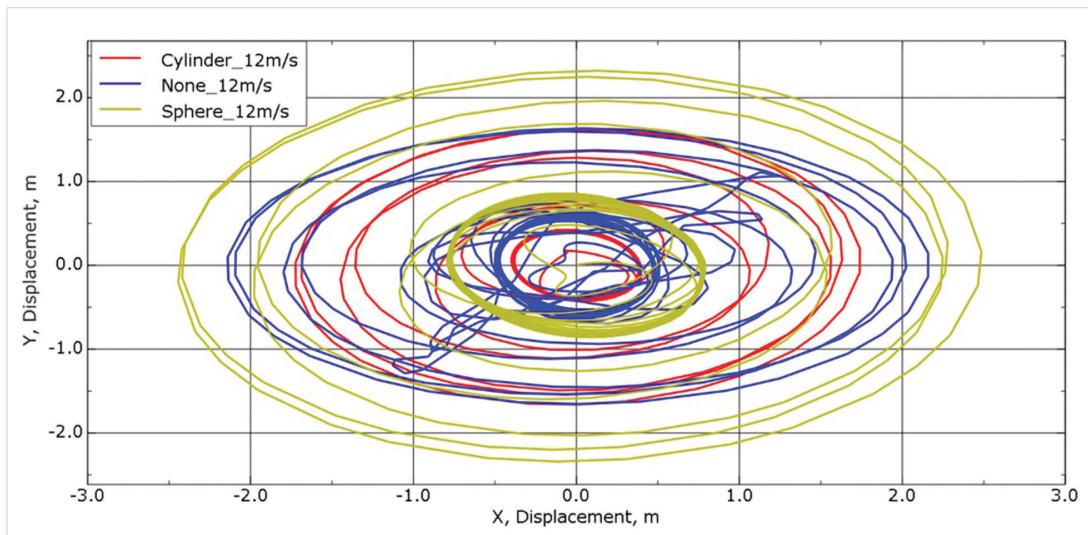


Figure 12 Movement trajectories of hook blocks in different variants for a wind speed of 12 m/s.  
 Slika 12. Putanje gibanja koloturника kuke u različitim varijantama za brzinu vjetrova od 12 m/s

Source: Authors

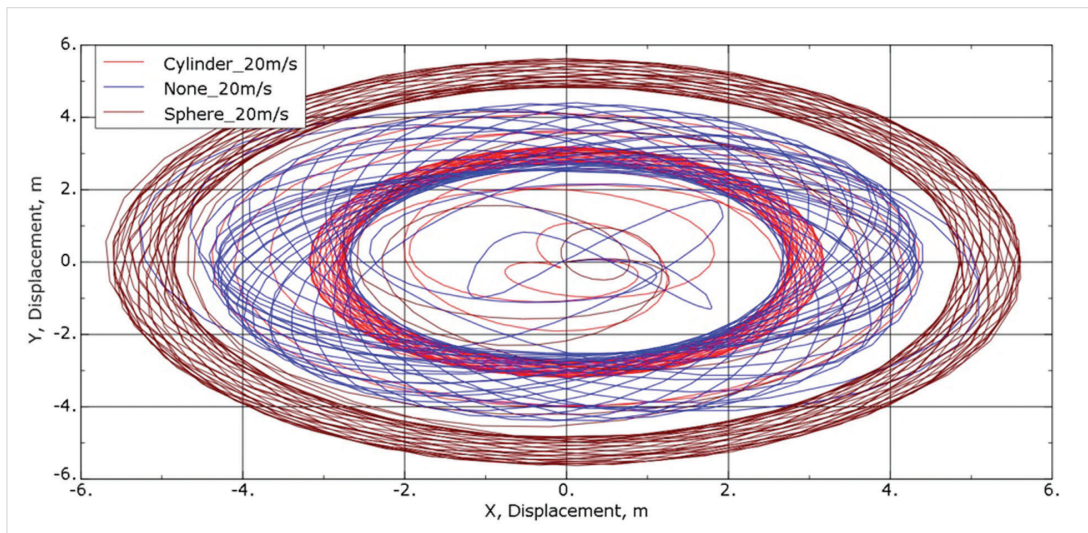


Figure 13 Movement trajectories of hook blocks in different variants for a wind speed of 20 m/s.  
 Slika 13. Putanje gibanja koloturника kuke u različitim varijantama za brzinu vjetrova od 20 m/s

Source: Authors

The figures below compare (Figure 12, Figure 13) the block trajectories depending on the type of fairing used and two wind speeds of 12 m/s and 20 m/s.

The drawings show that using different fairings will allow obtaining different pulley trajectories. Differences are visible depending on the design solution used, both in the deflection amplitude and the exact trajectory.

Moreover, the pulley trajectories were compared with each other depending on the wind speed, using the identical fairings.

Based on the simulations, it can be seen that the block trajectories depend on the input. This is due to the interference between the loads and the pendulum response. The presented trajectories should be compared with the experiment and a thorough mathematical analysis as mentioned in [12] should be carried out, which is planned to be performed as part of further work.

## 6. CONCLUSION / Zaključak

Based on the analysis, it can be concluded that:

- The use of FEM allows to determine the block trajectory using commercial code;
- The fairings have a significant influence on the block trajectory. Due to the lowest drag coefficient, the ball appears to be the most suitable shape as a fairing. However, a fairing in this shape increases the surface area affected by the wind. According to the analysis, the spherical deflector increases the deflection angles. The advantage of using deflectors is the systematization of the trajectory.
- The cylinder-shaped deflector has a similar advantage to a sphere. It increases the cross-sectional area affected by the wind, but not as much as a sphere. Analyses of the trajectories show that the cylinder-shaped fairing has the most significant impact on reducing the block deflection angle.

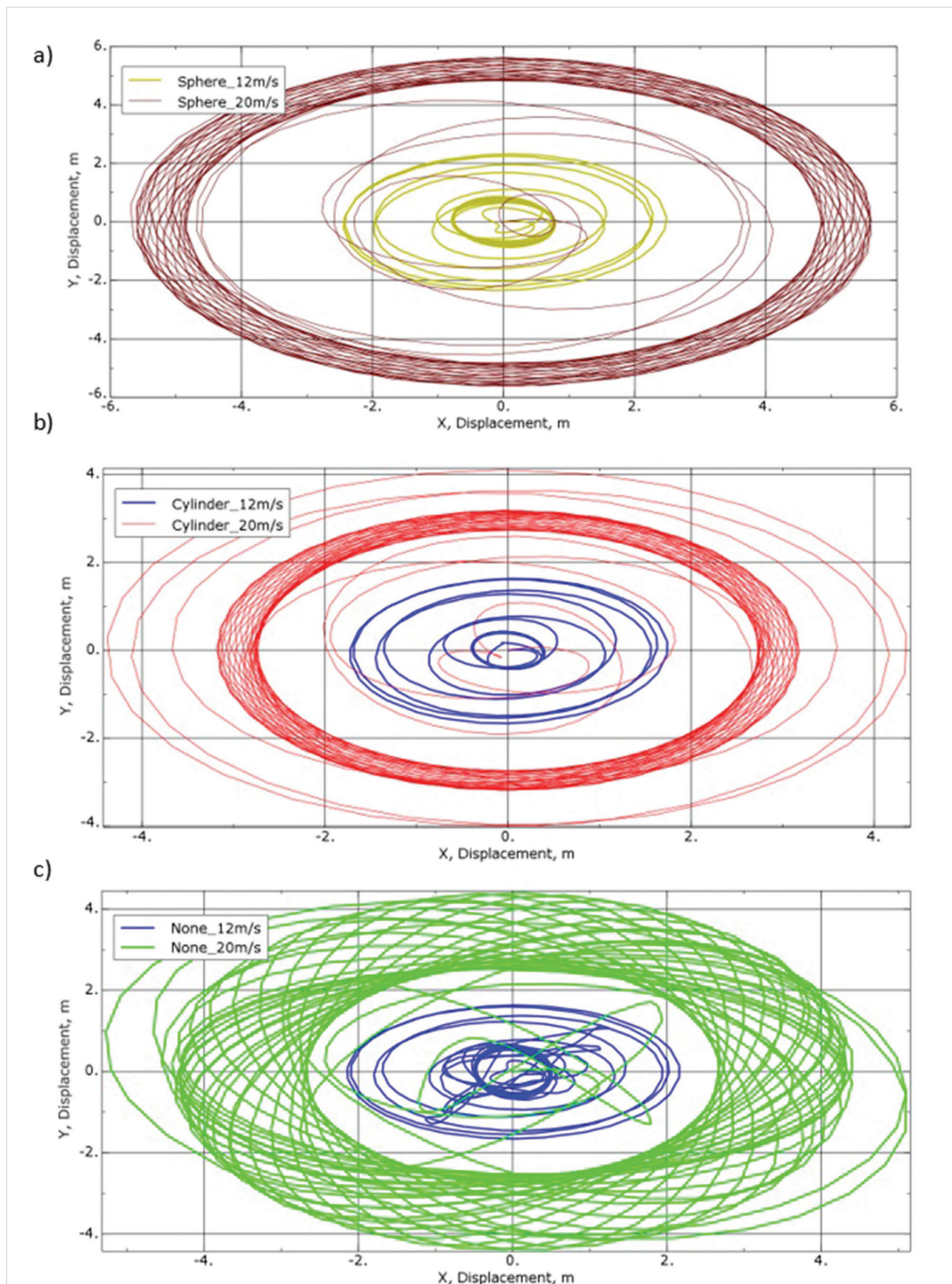


Figure 14 Block trajectories for the same fairings but different wind load speeds a) spherical cover, b) cylinder-shaped cover, c) without cover  
 Slika 14. Putanje koloturnika za iste oplate, ali različite brzine opterećenja vjetrova: a) sferični pokrov, b) pokrov cilindričnoga oblika, c) bez pokrova  
 Source: Authors

- The simulations do not consider the frictional forces in the block bearings or the air resistance to prevent the block from moving after the force is stopped. The only force that prevents the block from moving is gravity. The analyze of the block movement in more detail, model block mounting and air resistance should be analyzed after the force has ceased to be modelled. Such a task is more complicated and may be considered in later studies.
- The use of cylindrical fairings on the blocks of cranes operating in ports can significantly facilitate the work of loading and prevent accidents related to the inertia of the hook block when suspending the load.

## REFERENCES / Literatura

- [1] PGE Baltica zakończyła badania wietrzności na Bałtyku. (2020, luty 11). *BiznesAlert.pl*. <https://biznesalert.pl/pge-baltica-morskie-farmy-wiatrowe-wietrzność-energetyka/>
- [2] MacCrimmon, R. A. (2005). *Guide for the design of crane-supporting steel structures*. Canadian Institute of Steel Construction = Institut canadien de la construction en acier.
- [3] Standards Australia, 01/29/2021. (b. d.). *AS 1418.1-1994: Cranes. Part 1: General requirements*.
- [4] Rowswell, J. C. (b. d.). *Crane runway systems*. University of Toronto.
- [5] TR244C. (2002). *Hoisting and Rigging Fundamentals for Riggers and Operators*, Rev. 5.
- [6] Piskur, P.; Szymak, P.; Larzewski, B. (2021). "Shipyard Crane Modeling Methods". *Pedagogika - Pedagogy*, Vol. 93 (6s), pp. 279-290. <https://doi.org/10.53656/ped21-6s.25shi>

- [7] Ricker, D. T. (1982). "Tips for avoiding crane runway problems". *Engineering Journal*, pp. 181-205.
- [8] Charchalis, A. (2001). *Opory okrętów wojennych i pędniki okrętowe [Resistance force of warships and ship propellers]*. Akademia Marynarki Wojennej im. Bohaterów Westerplatte.
- [9] Baker, W. E.; Cox, P. A.; Westine, P. S.; Kulesz, J. J.; Strehlow, R. A. (1983). *Explosion hazards and evaluation*. Elsevier.
- [10] Emerson, A. W. (2006). "Things are seldom what they seem: Christiaan Huygens, the Pendulum, and the Cycloid". *Undefined*. [https://doi.org/10.1097/00000542-196809000-00002](https://www.semantic-scholar.org/paper/Things-are-seldom-what-they-seem%3A-Christiaan-the-Emmerson/086557ae105796127063e69807b340512646dbd3)
- [11] Szymak, P.; Piskur, P.; Goszczyński, J.; Batur, T. (2021). "Measurement Of The Dynamics Of The Sheave Block Of Shipyard Crane With 1000 T Lifting Capacity For Verification Of The Laboratory Stand". *Pedagogika - Pedagogy*, Vol. 93 (7s), pp. 96-109. <https://doi.org/10.53656/ped21-7s.08meas>
- [12] Marchel, Ł.; Specht, C.; Specht, M. (2020). "Assessment of the Steering Precision of a Hydrographic USV along Sounding Profiles Using a High-Precision GNSS RTK Receiver Supported Autopilot". *Energies*, Vol. 13, No. 21, p. 5637 <https://doi.org/10.3390/en13215637>